The Cryosphere Discuss., 4, 2483–2512, 2010
www.the-cryosphere-discuss.net/4/2483/2010/
doi:10.5194/tcd-4-2483-2010

The Cryosphere Discussions

Northern Hemisphere spring snow cover variability and change over 1922–2010 including an assessment of uncertainty

R. D. Brown[1] and D. A. Robinson[2]

[1]Climate Processes Section, Climate Research Division, Environment Canada @ Ouranos, 550 Sherbrooke St. West, 19th Floor, Montréal, QC, H3A 1B9, Canada
[2]Department of Geography, Rutgers University, 54 Joyce Kilmer Avenue Piscataway, NJ 08854-8054, USA

Received: 5 November 2010 – Accepted: 10 November 2010 – Published: 24 November 2010

Correspondence to: R. D. Brown (ross.brown@ec.gc.ca)

Published by Copernicus Publications on behalf of the European Geosciences Union.

Abstract

An update is provided of Northern Hemisphere (NH) spring (March, April) snow cover extent (SCE) over the 1922–2010 period incorporating the new climate data record (CDR) version of the NOAA weekly SCE dataset, with annual 95% confidence intervals estimates from regression analysis and intercomparison of multiple datasets. The uncertainty analysis indicated a 95% confidence interval in NH spring SCE of ±5–10% over the pre-satellite period and ±3–5% over the satellite era. The multi-dataset analysis showed there are larger uncertainties monitoring spring SCE over Eurasia (EUR) than North America (NA) due to the more complex regional character of the snow cover variability with the largest dataset uncertainty located over eastern Eurasia in a large region extending from the Tibetan Plateau across northern China.

Trend analysis of the updated SCE series provided evidence that NH spring snow cover extent has undergone significant reductions over the past ~90 years and that the rate of decrease has accelerated over the past 40 years. The rate of decrease in March and April NH SCE over the 1970–2010 period is ~7–8 million km^2 per 100 years which corresponds to an 8–11% decrease in NH March and April SCE respectively from pre-1970 values. In March, most of the change is being driven by Eurasia (NA trends are not significant) but both continents exhibit significant SCE reductions in April.

The observed trends in SCE are consistent with recent warming trends over northern mid-latitude land areas with NH SCE exhibiting significant negative correlations to air temperature anomalies in March and April. The NH spring SCE-temperature sensitivity has remained relatively stable over the period of record although there is some evidence of contrasting changes in temperature sensitivity over both continents in April. There is evidence that changes in atmospheric circulation around 1980 involving the North Atlantic Oscillation and Scandinavian Pattern have contributed to reductions in March SCE over Eurasia.

1 Introduction

Reliable information on spatial and temporal variability in continental and hemispheric snow cover extent (SCE) is important for climate monitoring (e.g. Arndt et al., 2010), climate model evaluation (e.g. Foster et al., 1996; Frei et al., 2005; Roesch, 2006; Brown and Frei, 2007) and climate feedback studies (e.g. Hall and Qu, 2006; Fernandes et al., 2009). Previously published estimates of Northern Hemisphere (NH) monthly SCE used for evaluating climate models and monitoring variability and change in hemispheric SCE have typically been based on single datasets such as the National Ocean Atmospheric Administration (NOAA) weekly snow cover dataset (Robinson et al., 1993) or passive microwave-derived snow cover data (Armstrong and Brodzik, 2001) with little or no information on the likely range of uncertainty in the observations. Brown et al. (2010) showed there can be large differences in the amount of snow cover seen by different satellite sensors related to spatial resolution, cloud cover (for optical sensors) and wavelength specific interactions with the atmosphere, snowpack, terrain and land cover. Estimates of SCE derived from surface-based observations also have spatially and temporally varying uncertainties related to the uneven distribution of in situ observations.

Brown (2000) presented estimates of historical variability in NH March and April snow cover extent (SCE) over the 1922–1997 period that were subsequently updated and included in the 4th IPCC assessment (Lemke et al., 2007; Figs. SPM.3, TS.12 and 4.2). The 2007 update included an estimate of uncertainty derived from the interannual variability of the data series as no published estimates were available of the uncertainty in the in situ-based SCE reconstruction developed by Brown (2000) or in the NOAA satellite dataset used to monitor NH SCE since 1966 (Robinson et al., 1993). The fixed uncertainty interval applied in the IPCC report does not reflect the different uncertainty levels associated with the pre-satellite in situ-based SCE information, or improvements in snow mapping over the satellite era from increases in satellite resolution and frequency.

Brown et al. (2010) used a multi-dataset approach to estimate the observational uncertainty in Arctic spring SCE over the 1967–2008 period. This approach will be applied in this paper to provide estimates of the uncertainty in the NH spring SCE series presented in the 4th IPCC Assessment and to update the series using the new climate data record (CDR) version of the NOAA dataset (http://climate.rutgers.edu/snowcover). This version includes homogeneity corrections to account for a change in mapping procedures that took place in 1999 (Ramsay, 1998; Helfrich et al., 2007). The updated series (with estimated uncertainty levels) are used to document trends in NH spring SCE over the period from the early 1920s, and to examine associations with air temperature and atmospheric circulation.

2 Datasets

The various sources of snow cover data used in this study are summarized in Table 1. Detailed descriptions of these datasets are provided by Brown et al. (2010) and are not repeated here. The NH March and April SCE series presented in the 4th IPCC assessment were based on the historical snow cover index of Brown (2000) (henceforth defined as B2000) up to the start of the satellite era in the late-1960s, with SCE values after 1966 obtained from the NOAA weekly dataset (Robinson et al., 1993). The B2000 index was derived from reconstructed and observed daily snow depth over a fixed network of climate stations and is available over North America (NA) from 1915–1992 for the months of November to April, but is limited to October, March and April over Eurasia (EUR) for the 1922–1991 period due to a sparser network of observations. Consequently this dataset only provides hemispheric information in the months of March and April from 1922–1991. McCabe and Wolock (2010) reconstructed NH March SCE back to 1902 using gridded monthly temperature and precipitation data from the Climate Research Unit (CRU) in a simplified snow accumulation and melt model calibrated with the NOAA SCE dataset to define temperature thresholds for rain-snow probability and melt rate. The results agree reasonably closely with the B2000 series (not surprisingly since SCE and air temperature are strongly correlated over the NH in March) but the method is not considered to be particularly robust because of the monthly time-step, the use of non-physically based temperature thresholds, and the fact the method required calibration with the NOAA SCE series.

The NOAA dataset is based on weekly charts of snow cover extent derived from manual interpretation of visible satellite imagery up to 1999. The charting method changed in May 1999 with the introduction of the higher resolution 24 km daily Interactive Multi-Sensor (IMS) snow cover product (Ramsay, 1998). A pseudo-weekly product is automatically derived from the IMS 24 km daily product assuming the analysis for Sunday is representative of the previous week. This change was shown to map less snow in mountain regions than the manual analysis and has been corrected in the CDR version of the NOAA dataset. SCE was derived with the monthly version of the CDR dataset which gives the fraction of the month that snow cover was present. While efforts have been made to correct for changes in charting procedures in the CDR dataset, it is not possible to correct for any technological bias related to the increase in the volume and resolution of satellite information over time as well as variations in analyst experience and improvements in analysis tools.

The other datasets shown in Table 1 (B2003, CMC, ERA-40, ERA-40rec, NCEP, and PMW) were used to establish the confidence interval in March and April hemispheric SCE series as outlined in Sect. 3. The CMC and B2003 SCE series were combined (henceforth referred to as B2003+CMC) to provide additional NA monthly SCE series for estimating confidence intervals. These two datasets used different precipitation and temperature products to derive the first-guess snow depth field used in the optimal interpolation of surface snow depth observations but SCE should be largely insensitive to the background field in the November–April period when the snow line fluctuates across the mid-latitudinal zone of NA where there is a dense network of surface observations (Brown, 2000).

3 Methodology

The development of estimates of uncertainty in NH spring SCE series over the 1922–2010 period required the use of two different strategies based on the temporal distribution of the available datasets. For the earlier period of record where the only estimate was the B2000 snow cover index, the 95% confidence intervals were estimated from regression against the multi-dataset average anomaly over the 1967–1992 period of overlapping data using the regression forecast error method described in Sect. 3.1 below. The multi-dataset method outlined in Sect. 3.2 was used to estimate the confidence interval when there were at least 5 datasets available which coincided with the period 1967–2002. Confidence intervals in the period from 2003–2010 were estimated from the regression of NOAA against the CMC operational analysis over the 1998–2010 period of overlapping data; the CMC SCE estimates represent an independent source of SCE information that is highly correlated to the NOAA data set in March and April (see bottom row Table 2) when the snow line is located where the observing network is relatively dense. The B2000 and NOAA datasets were retained as the base series for applying the confidence intervals to maintain the continuity of the series presented in Brown (2000) and the 4th IPCC Assessment, and because there is greater confidence in the homogeneity of these series.

3.1 Regression-based estimate of confidence interval

Regression analysis was used to estimate the confidence interval from the standard error of forecast (SE_f) when there were insufficient datasets to compute a multi-dataset estimate of the confidence interval. SCE series were converted to standardized anomalies with respect to the period of the regression analysis which makes the error analysis insensitive to the choice of dependent and independent variables, and reduces the computation of SE_f in each year to Eq. (1) as the anomaly series has a

Discussion Paper | Discussion Paper | Discussion Paper | Discussion Paper |

standard deviation of 1, and the mean and sum of the anomaly series are both 0.

$$\mathrm{SE_f} = \mathrm{SE_{res}}\sqrt{(1 + (1/n)(1 + x_i^2))}, \tag{1}$$

where $\mathrm{SE_{res}}$ is the standard error of the residuals from the best fit line, x_i is the standardized anomaly of the independent variable in year i, and n is the number of pairs of anomalies included in the regression analysis. A 95% confidence interval is then obtained from $\pm\, t_\mathrm{c}\, \mathrm{SE_f}$ where t_c is the Students t-statistic corresponding to 0.05 level of significance for $n-1$ degrees of freedom. An estimate of the root mean squared error in the dependent data was obtained from a standard leave-one-out cross-validation (LOOCV) analysis.

3.2 Multi-dataset estimate of confidence interval

Confidence intervals were estimated from the standard error of the multiple datasets over the 1967–2002 period when there were at least five datasets available in any given year. The five dataset minimum was imposed to reduce variability due to sample size. The datasets available in this period were B2000 (up to 1992), B2003+CMC (NA only from 1979), ERA-40, ERA-40rec, NCEP, NOAA, and PMW. Datasets were converted to standardized anomalies for a 1979–2002 reference period and an estimate of the confidence interval in monthly SCE obtained from the standard error (SE) of the average multi-dataset standardized anomaly series computed from

$$\mathrm{SE} = s/\sqrt{(n-1)}, \tag{2}$$

which depends on the standard deviation, s, of the n datasets included in the average anomaly. The 95% confidence interval was then computed from $\pm\, t_\mathrm{c}$ SE where t_c is Students t-statistic corresponding to 0.05 level of significant for $n-1$ degrees of freedom. The B2000 series was padded with values estimated from regression against the NOAA dataset for the 1993 to 2002 period to convert the series to anomalies with respect to the 1979–2002 reference period. The error estimates were converted back

to SCE in units of $10^6\,\mathrm{km}^2$ using the reference period mean and standard deviation from the NOAA dataset.

An evaluation of the degree of consistency between datasets in March–April was carried out as part of the multi-dataset uncertainty analysis over two periods of dataset overlap: 1959–1991, and 1979–2002. This included the correlation and root mean square difference between detrended SCE anomalies for each dataset and the multi-dataset average anomaly series (excluding the dataset being evaluated).

4 Results

4.1 Dataset evaluation

The dataset evaluation results for March and April separated by continent (Table 2) show a clear contrast in dataset consistency between the two continents in April with most datasets exhibiting closer agreement over NA than EUR. The NOAA dataset is a case in point; it had the lowest agreement with the multi-dataset average over EUR in March–April in the 1979–2002 overlap period but had comparable correlations to the other datasets over NA in the same period. The reason for the overall greater dataset consistency over NA is likely related to the more regionally constrained character of the continental snow cover variability compared to EUR which is clearly seen in the principal component analysis of NH SCE variability provided by Frei and Robinson (1999). Other noteworthy points are the generally strong performance of the in situ based estimates of SCE (B2000 and B2003+CMC) and the fact that downscaling SCE from ERA-40 temperature and precipitation provided superior results than SCE derived from ERA-40 snow depth fields. There was no evidence of any systematic trends or step changes in the difference series between NOAA and the multi-dataset average in March and April over the 1967 to 2002 period (not shown) confirming the work by the Rutgers Global Snow Lab to maintain the homogeneity of the NOAA snow cover series.

To gain further insight into the spatial pattern of between dataset variability, mean March and April snow cover fraction observed over the 1979–2002 dataset overlap period (see Table 2 for list of datasets) were interpolated to a common 190.5 km polar stereographic grid and the standard deviation contoured (Fig. 1). The results confirm the larger between-dataset variability over Eurasia noted above and show that differences are largest over a broad swath of eastern Eurasia extending from the Tibetan Plateau across northern China. The larger dataset variability in this region is related to a number of factors that variously influence every dataset included in the analysis including complex topography and transient snow cover anomalies (implications for the resolution and frequency of observations), a lack of real-time surface observations (B. Brasnett, personal communication, 2010), difficulties with passive microwave snow cover retrieval algorithms related to topography and atmospheric effects (e.g. Savoie et al., 2009), and challenges simulating atmospheric circulation interactions with the Tibetan Plateau (e.g. Cui et al., 2007; Randall et al., 2007).

4.2 Confidence interval

The results of the confidence interval analysis for March and April SCE are shown in Fig. 2 for both continents. The values are smoothed with a 13-term binomial filter to facilitate the comparison as the estimated confidence intervals from the multi-dataset method can vary greatly from one year to the next. The uncertainty is highest in the period prior to 1967 when the estimate is based solely on the regression analysis and decreases rapidly over the 1970s and 1980s in response to an increase in the number of datasets and increased frequency and resolution of snow cover information. The larger confidence interval for Eurasia April SCE is evident reflecting the larger inconsistencies between datasets noted previously. The confidence limits are shown in Fig. 3 for NH SCE expressed as percentages of monthly SCE. These range from ±5% to ±9% for March and April SCE over the early period of record to ±3% to ±5% over the more recent period of satellite-based observations.

4.3 Analysis of updated SCE series including estimated confidence interval

The estimated confidence intervals were applied to the merged B2000 and NOAA SCE anomaly series to update the SCE series published in Brown (2000) (Fig. 4). The final NH series were converted to SCE in million km^2 using the 1979–2002 reference period mean and standard deviation from the NOAA dataset (Fig. 5). A 13-term binomial filter was applied to remove fluctuations on less than decadal time scales following the approach used in the 4th IPCC Assessment (Trenberth et al., 2007, Appendix 3.A). The updated anomaly series in Fig. 4 show that NA March SCE increased over the first half of the 20th C followed by a period of rapid decrease in the late-1980s and early-1990s that rebounded slightly during the late-1990s. Over Eurasia, March SCE has remained more or less stable from the 1920s up to the end of the 1980s when SCE underwent a similar rapid step decrease as NA to lower values that have remained more or less constant since. The NA April SCE series shows some similarity to March with the notable point that the 2010 anomaly is the lowest in the 96 year period (the second warmest April over NA mid-latitudes after 1987 based on air temperature anomalies averaged over 40–60° N for each continent from the CRUTEM3 dataset of Brohan et al., 2006). Eurasian April SCE differs from NA with more evidence of long-term decreases over the entire period of record. The rapid reductions in SCE in the late-1980s and early 1990s seen in both continents in March and April coincide with a change in NH circulation patterns to more positive values of the North Atlantic and Arctic Oscillations (Watanabe and Nitta, 1999; Overland et al., 1999).

Analysis of secular variability in the relationship between winter (January–March) values of the leading 10 modes of NH atmospheric variability computed by the Climate Prediction Center (http://www.cpc.noaa.gov/data/teledoc/telecontents.shtml) and NH SCE with 21-year running correlations over the period from 1951–2010 showed evidence of an abrupt strengthening of the relationship between the North Atlantic Oscillation (NAO) and NH March SCE around1980, and an increase in the importance of the Scandinavian (SCA) pattern over the period after the mid-1980s (Fig. 6). The

SCA pattern (originally referred to as the Eurasia-1 pattern by Barnston and Livezey, 1987) describes the strength of the quasi-permanent ridge of winter high pressure over Scandinavia and northern Europe and positive (negative) values of SCA contribute to cold (warm) March temperature anomalies over central Eurasia and to a lesser extent over the United States (Fig. 7 left panel). NAO has been shown to be a significant factor in winter precipitation and snow cover variability across western Europe and eastern North America (Gutzler and Rosen, 1992; Clark et al., 1999; Bednorz, 2004; Henderson and Leathers, 2010) and positive (negative) values of NAO contribute to warm (cold) March temperature anomalies over central Eurasia (Fig. 7 right panel). Prior to the mid-1980s NAO and SCA were not significantly correlated but since then the two patterns exhibit a significant negative correlation that reinforces the influence on winter temperature anomalies and SCE. The two patterns have also tended to be in modes that favor warm winter temperature anomalies over most of the period since 1980 (Fig. 8). The same analysis for April (not shown) revealed similar evidence of an increase in the importance of NAO around 1980 but the correlations were much weaker than March and ceased to be statistically significant after about 1990. There were no sustained significant correlations between April SCE and the SCA index over the 1951–2010 period. While atmospheric circulation may be playing a role in some of the recent decreases, long-term changes in air temperature are definitely calling the tune with NH mid-latitude air temperatures explaining ~50% of the variance in NH spring snow cover over the 89-year period analyzed (Fig. 9).

Results of linear trend analysis including annual estimates of error in SCE are shown in Table 3 for the entire data period as well as for the more recent period of satellite data from 1970. The results show greater evidence of systematic decreases in continental spring SCE than the trends published in Brown (2000) with NH March and April SCE both exhibiting significant (0.05 level) negative trends over the period from 1922–2010. The rates of decrease are much higher when computed over the period of satellite coverage as the data start during a period when hemispheric snow cover was relatively high, and include the period of recent rapid warming.

The temperature sensitivity values for the updated NH spring SCE series were computed using March and April monthly temperature anomaly series from the CRUTEM3 dataset averaged over NH land areas between 40 and 60° N following Brown (2000) (Table 4). A least-squares regression method was used that included the annual estimates of observational errors in SCE. The results obtained with the updated NH series with annual error estimates included are $-1.44 \times 10^6\,\mathrm{km^2\,°C^{-1}}$ ($r^2 = 0.50$) and $-2.00 \times 10^6\,\mathrm{km^2\,°C^{-1}}$ ($r^2 = 0.49$) for March and April respectively which are similar to the values published in Brown (2000) except that temperature explains a larger fraction of the variance with the updated series. A comparison of the air temperature sensitivities computed over the pre- and post-satellite periods of data record for each continent separately (Table 4) showed that SCE temperature sensitivity in April has increased significantly over NA in the period since 1970 while it has decreased significantly over Eurasia. The reasons for these changes are difficult to diagnose as they could be generated by any number of causes including shifts in snowlines, changes in atmospheric circulation, changes in spring snow depths, and changes in surface or snow albedo. A number of Russian authors have reported significant increases in winter snow accumulation over large areas of Eurasia (Bulygina et al., 2009; Shmakin, 2010) that contrast with trends toward generally shallower winter snow cover over Canada (Brown and Braaten, 1998; Kitaev et al., 2005). Everything being equal, shallower snowpacks will respond more quickly to temperature anomalies so the difference in recent winter snow accumulation trends between the two continents may be playing a role. The temperature sensitivity results shown in Table 4 suggest that EUR will dominate the NH SCE response to warming in March, while the April response will have important contributions from both continents.

5 Summary and conclusions

An update to the NH spring SCE series used in the 4th IPCC Assessment (Lemke et al., 2007) is provided based on the B2000 index and the latest CDR version of the NOAA weekly SCE dataset with annual error estimates obtained from regression analysis and intercomparison of multiple datasets. The analysis revealed that the 95% confidence interval in NH spring SCE are in the ±5–10% range over the pre-satellite period and ±3–5% over the satellite era. The multi-dataset analysis indicated there are larger uncertainties monitoring spring SCE over Eurasia than NA which is considered to be related in part to the more complex regional character of snow cover variability over Eurasia and major challenges monitoring snow cover over the Tibetan Plateau region.

Trend analysis of the updated SCE series provided evidence that NH spring snow cover extent has undergone significant reductions over the past ~90 years and that the rate of decrease has accelerated over the past 40 years. The rate of decrease in March and April NH SCE over the 1970–2010 period is ~7–8 million km^2 per 100 years which corresponds to an 8–11% decrease in NH March and April SCE respectively from pre-1970 values. In March, most of the change is being driven by Eurasia (NA trends are not significant) but both continents exhibit significant reductions in April SCE.

The observed trends in SCE are consistent with recent warming trends over northern mid-latitude land areas with NH SCE exhibiting significant negative correlations to air temperature anomalies in March and April. The NH spring SCE-temperature sensitivity has remained relatively stable over the period of record although there is some evidence of contrasting changes in temperature sensitivity over both continents in April. There is also evidence that changes in atmospheric circulation around 1980 involving the NAO and SCA patterns have contributed to reductions in March SCE over Eurasia.

Acknowledgements. The authors thank Mary-Jo Brodzik (NSIDC) for supplying the PMW dataset and Bruce Brasnett (CMC) for the CMC global daily snow depth analysis. ECMWF are acknowledged for providing the ERA-40 data used in this study through the ECMWF data server (http://data.ecmwf.int/data/). NCEP data were provided by the Physical Sciences Division, Earth System Research Laboratory, NOAA, Boulder, Colorado (http://www.esrl.noaa.gov/psd/). Chris Derksen (Env. Canada) and Gina R. Henderson (Rutgers University) are gratefully acknowledged for helpful comments on the draft manuscript. D. Robinson acknowledges funding support from NASA MEaSURES award NNX08AP34A and NOAA Climate Program Office

awards EA133E10SE2623 and NA08AR4310678. Cathy Smith of the NOAA Earth System Research Laboratory is acknowledged for her work in developing and maintaining the online analysis and plotting tools for NCEP Reanalysis output.

References

Armstrong, R. L. and Brodzik, M. J.: Recent Northern Hemisphere snow extent: a comparison of data derived from visible and microwave sensors, Geophys. Res. Lett., 28, 3673–3676, 2001.

Arndt, D. S., Baringer, M. O., and Johnson, M. R.: State of the Climate in 2009, B. Am. Meteorol. Soc., 91, S1–S222, doi:10.1175/BAMS-91-7-StateoftheClimate, 2009.

Barnston, A. G. and Livezey, R. E.: Classification, seasonality and persistence of low-frequency atmospheric circulation patterns, Mon. Weather Rev., 115, 1083–1126, 1987.

Bednorz, E.: Snow cover in Eastern Europe in relation to temperature, precipitation and circulation, Int. J. Climatol., 24, 591–601, 2004.

Brasnett, B.: A global analysis of snow depth for numerical weather prediction, J. Appl. Meteorol., 38, 726–740, 1999.

Brohan, P., Kennedy, J. J., Harris, I., Tett, S. F. B., and Jones, P. D.: Uncertainty estimates in regional and global observed temperature changes: a new dataset from 1850, J. Geophys. Res., 111, D12106, doi:10.1029/2005JD006548, 2006.

Brown, R. D.: Northern Hemisphere snow cover variability and change, 1915–1997, J. Climate, 13, 2339–2355, 2000.

Brown, R. D. and Braaten, R. O.: Spatial and temporal variability of Canadian monthly snow depths, 1946–1995, Atmos. Ocean, 36, 37–45, 1998.

Brown, R. D. and Frei, A.: Comment on "Evaluation of surface albedo and snow cover in AR4 coupled models" by Roesch, A., J. Geophys. Res., 112, D22102, doi:10.1029/2006JD008339, 2007.

Brown, R. D., Brasnett, B., and Robinson, D.: Gridded North American monthly snow depth and snow water equivalent for GCM evaluation, Atmos. Ocean, 41, 1–14, 2003.

Brown, R., Derksen, C., and Wang, L.: A multi-data set analysis of variability and change in Arctic spring snow cover extent, 1967–2008, J. Geophys. Res., 115, D16111, doi:10.1029/2010JD013975, 2010.

Bulygina, O. N., Razuvaev, V. N., and Korshunova, N. N.: Changes in snow cover over Northern Eurasia in the last few decades, Environ. Res. Lett., 4, 045026, doi:10.1088/1748-9326/4/4/045026, 2009.
Clark, M. P, Serreze, M. C., and Robinson, D. A.: Atmospheric controls on Eurasian snow cover extent, Int. J. Climatol., 19, 27–40, 1999.
Cui, X., Langmann, B., and Graf, H.-F.: Summer monsoonal rainfall simulation on the Tibetan Plateau with a Regional Climate Model using a one-way double-nesting system, SOLA, 3, 049052, doi:10.2151/sola.2007013, 2007.
Fernandes, R., Zhao, H., Wang, X., Key, J., Qu, X., and Hall, A.: Controls on Northern Hemisphere snow albedo feedback quantified using satellite Earth observations, Geophys. Res. Lett., 36, L21702, doi:10.1029/2009GL040057, 2009.
Foster, J., Liston, G., Koster, R., Essery, R., Behr, H., Dumenil, L., Verseghy, D., Thompson, S., Pollard, D., and Cohen, J.: Snow cover and snow mass intercomparisons of general circulation models and remotely sensed datasets, J. Climate, 9, 409–426, 1996.
Frei, A. and Robinson, D. A.: Northern Hemisphere snow extent: regional variability 1972–1994, Int. J. Climatol., 19, 1535–1560, 1999.
Frei, A., Hughes, M. G., and Robinson, D. A.: North American snow extent: 1910–1994, Int. J. Climatology, 19, 1517–1534, 1999.
Frei, A., Brown, R., Miller, J. A., and Robinson, D. A.: Snow mass over North America: observations and results from the second phase of the Atmospheric Model Intercomparison Project (AMIP-2), J. Hydrometeorol., 6, 681–695, 2005.
Gutzler, D. S. and Rosen, R. D.: Interannual variability of wintertime snow cover across the Northern Hemisphere, J. Climate, 5, 441–1447, 1992.
Hall, A. and Qu, X.: Using the current seasonal cycle to constrain snow albedo feedback in future climate change, Geophys. Res. Lett., 33, L03502, doi:10.1029/2005GL025127, 2006.
Helfrich, S. R., McNamara, D., Ramsay, B. H., Baldwin, T., and Kasheta, T.: Enhancements to, and forthcoming developments in the Interactive Multisensor Snow and Ice Mapping System (IMS), Hydrol. Process., 21, 1576–1586, 2007.
Henderson, G. and Leathers, D.: European snow cover extent variability and associations with atmospheric forcings, Int. J. Climatol., 30, 1440–1451, doi:10.1002/joc.1990, 2010.
Kalnay, E., Kanamitsu, M., Kistler, R., Collins, W., Deaven, D., Gandin, L., Iredell, M., Saha, S., White, G., Woollen, J., Zhu, Y., Chelliah, M., Ebisuzaki, W., Higgins, W., Janowiak, J., Mo, K. C., Ropelewski, C., Wang, J., Leetmaa, A., Reynolds, R., Jenne, R., and Joseph, D.: The

NCEP/NCAR Reanalysis Project, B. Am. Meteorol. Soc., 77, 437–471, 1996.
Kitaev, L., Førland, E., Razuvaev, V., Tveito, O. E., and Krueger, O.: Distribution of snow cover over Northern Eurasia, Nord. Hydrol., 36, 311–319, 2005.
Lemke, P., Ren, J., Alley, R. B., Allison, I., Carrasco, J., Flato, G., Fujii, Y., Kaser, G., Mote, P., Thomas, R. H., and Zhang, T.: Observations: Changes in Snow, Ice and Frozen Ground, in: Climate Change 2007: The Physical Science Basis. Contribution of Working Group I to the Fourth Assessment Report of the Intergovernmental Panel on Climate Change, edited by: Solomon, S., Qin, D., Manning, M., Chen, Z., Marquis, M., Averyt, K. B., Tignor, M., and Miller, H. L., Cambridge University Press, Cambridge, United Kingdom and New York, NY, USA, 2007.
McCabe, G. J. and Wolock, D. M.: Long-term variability in Northern Hemisphere snow cover and association with warmer winters, Climatic Change, 99, 141–153, 2010.
Overland, J. E., Adams, J. M., and Bond, N. A.: Decadal variability of the Aleutian Low and its relation to high-latitude circulation, J. Climate, 12, 1542–1548, 1999.
Ramsay, B.: The interactive multisensor snow and ice mapping system, Hydrol. Process., 12, 1537–1546, 1998.
Randall, D. A., Wood, R. A., Bony, S., Colman, R., Fichefet, T., Fyfe, J., Kattsov, V., Pitman, A., Shukla, J., Srinivasan, J., Stouffer, R. J., Sumi, A., and Taylor, K. E.: Climate models and their evaluation, in: Climate Change 2007: The Physical Science Basis. Contribution of Working Group I to the Fourth Assessment Report of the Intergovernmental Panel on Climate Change, edited by: Solomon, S., Qin, D., Manning, M., Chen, Z., Marquis, M., Averyt, K. B., Tignor, M., and Miller, H. L., Cambridge University Press, Cambridge, United Kingdom and New York, NY, USA, 2007.
Robinson, D. A., Dewey, K. F., and Heim, R. R.: Global snow cover monitoring: an update, B. Am. Meteorol. Soc., 74, 1689–1696, 1993.
Roesch, A.: Evaluation of surface albedo and snow cover in AR4 coupled climate models, J. Geophys. Res., 111, D15111, doi:10.1029/2005JD006473, 2006.
Savoie, M. H., Armstrong, R. L., Brodzik, M. J., and Wang, J. R.: Atmospheric corrections for improved passive microwave snow cover retrievals over the Tibet Plateau, Remote Sens. Environ., 113, 2661–2669, 2009.
Shmakin, A. B.: Climatic characteristics of snow cover over North Eurasia and their change during the last decades, Ice and Snow, 1, 43–57, 2010 (in Russian with English summary).
Trenberth, K. E., Jones, P. D., Ambenje, P., Bojariu, R., Easterling, D., Tank, A. K., Parker,

D., Rahimzadeh, F., Renwick, J. A., Rusticucci, M., Soden, B., and Zhai, P.: Observations: Surface and Atmospheric Climate Change, in: Climate Change 2007: The Physical Science Basis. Contribution of Working Group I to the Fourth Assessment Report of the Intergovernmental Panel on Climate Change, edited by: Solomon, S., Qin, D., Manning, M., Chen, Z., Marquis, M., Averyt, K. B., Tignor, M., and Miller, H. L., Cambridge University Press, Cambridge, United Kingdom and New York, NY, USA, 2007.

Uppala, S. M., Kållberg, P. W., Simmons, A. J., Andrae, U., da Costa Bechtold, V., Fiorino, M., Gibson, J. K., Haseler, J., Hernandez, A., Kelly, G. A., Li, X., Onogi, K., Saarinen, S., Sokka, N., Allan, R. P., Andersson, E., Arpe, K., Balmaseda, M. A., Beljaars, A. C. M., van de Berg, L., Bidlot, J., Bormann, N., Caires, S., Chevallier, F., Dethof, A., Dragosavac, M., Fisher, M., Fuentes, M., Hagemann, S., Hólm, E., Hoskins, B. J., Isaksen, L., Janssen, P. A. E. M., Jenne, R., McNally, A. P., Mahfouf, J.-F., Morcrette, J.-J., Rayner, N. A., Saunders, R. W., Simon, P., Sterl, A., Trenberth, K. E., Untch, A., Vasiljevic, D., Viterbo, P., and Woollen, J.: The ERA-40 re-analysis, Q. J. Roy. Meteor. Soc., 131, 2961–3012, doi:10.1256/qj.04.176, 2005.

Watanabe, M. and Nitta, T.: Decadal changes in the atmospheric circulation and associated surface climate variations in the northern hemisphere winter, J. Climate, 12, 494–510, 1999.

Table 1. Summary of data sources used in the analysis.

Acronym	Dataset Description	Period	Resolution	Data Source
B2000	Monthly snow cover index for NA and Eurasia based on gridded observed and reconstructed daily snow depth at surface climate stations	NA, 1915–1992 EUR, 1922–1991	190.5 km	Brown (2000)
B2003	Daily snow depth analysis over NA from optimal interpolation of historical in situ snow depth observations	1979–1997	~35 km	Brown et al. (2003)
CMC	Canadian Meteorological Centre global daily snow depth analysis from optimal interpolation of real-time in situ observations	1998–2010	~35 km	National Snow and Ice Data Center (NSIDC), Brasnett (1999)
ERA-40	ERA-40 reanalysis daily snow depths	1957–2002	~275 km	European Centre for Medium-Range Weather Forecasts (ECMWF), Uppala et al. (2005).
ERA-40rec	ERA-40 reconstructed snow cover duration with temperature-index snow model of Brown et al. (2003)	1957–2002	~275 km (with 5 km empirical elevation adjustment)	Brown et al. (2010)
NCEP	Snow cover proxy derived from National Centers for Environmental Prediction Reanalysis daily temperatures (land area inside the 0 °C isotherm)	1948–2008	~275 km	Brown et al. (2010), Earth System Research Laboratory, NOAA, Kalnay et al. (1996)
NOAA	National Oceanic and Atmospheric Administration weekly snow/no-snow charts	1966–2010	190.5 km	Rutgers U., Robinson et al. (1993)
PMW	Snow water equivalent from Scanning Multichannel Microwave Radiometer (SMMR, 1978–1987) and the Special Sensor Microwave/Imager (SSM/I, 1987–2008)	1978–2008	24 km	NSIDC, Savoie et al. (2009)

Table 2. Correlation and root mean square differences (rmsd) in detrended SCE anomalies versus the multi-dataset average anomaly (excluded the dataset being evaluated) in three periods of data overlap. The units of rmsd are dimensionless (standardized anomalies). The correlations and rmsd (from LOOCV) are also shown for the regression analyses used to estimate the confidence interval in B2000 prior to 1967 and for NOAA after 2002. All correlations are statistically significant at the 0.05 level.

	North America				Eurasia			
	March		April		March		April	
	r	rmsd	*r*	rmsd	*r*	rmsd	*r*	rmsd
Dataset overlap period: 1959–1991								
B2000	0.87	0.45	0.90	0.41	0.85	0.53	0.78	0.61
ERA-40	0.73	0.67	0.83	0.53	0.86	0.49	0.72	0.68
ERA-40rec	0.81	0.56	0.92	0.37	0.95	0.30	0.91	0.42
NCEP	0.67	0.73	0.77	0.61	0.87	0.50	0.78	0.56
Dataset overlap period: 1979–2002								
B2003+CMC	0.95	0.33	0.91	0.38	n/a		n/a	
ERA-40	0.66	0.75	0.84	0.53	0.87	0.40	0.81	0.54
ERA-40rec	0.87	0.48	0.91	0.41	0.89	0.37	0.84	0.45
NCEP	0.72	0.68	0.91	0.39	0.80	0.51	0.91	0.44
NOAA	0.84	0.54	0.90	0.43	0.65	0.65	0.62	0.74
PMW	0.88	0.42	0.86	0.47	0.77	0.60	0.70	0.71
Regression analysis results for B2000 versus multi-dataset for 1967–1992 period	0.94	0.28	0.91	0.34	0.91	0.34	0.84	0.48
Regression analysis results for NOAA versus CMC for 1998–2010 period	0.97	0.22	0.99	0.16	0.98	0.18	0.91	0.43

Table 3. Summary of linear least-squares regression trend analysis results including annual error estimates. Trends significant at a 0.05 level are indicated with asterisks. The units are $10^6\,km^2\,(100\,yr)^{-1}$.

Region	March	April
North America		
1915–2010	−0.22	−0.83*
1970–2010	−0.77	−3.77*
Eurasia		
1922–2010	−3.20*	−1.17*
1970–2010	−4.83*	−5.33*
Northern Hemisphere		
1922–2010	−3.24*	−4.72*
1970–2010	−7.26*	−8.30*

Discussion Paper | Discussion Paper | Discussion Paper | Discussion Paper |

Table 4. Summary of regression analysis between continental and hemispheric monthly SCE and air temperature anomalies over land areas between 40–60° N from the CRU dataset. Units are $10^6\,km^2\,C^{-1}$. The fraction of the variance explained by the regression is shown in parentheses. Statistically significant (0.05 level) values are indicated with a single asterisk while a second asterisk denotes the slopes are also significantly different between the two periods before and after 1970.

Region	March	April
North America		
1922–1969	−0.46* (0.38)	−0.62* (0.48)
1970–2010	−0.36* (0.32)	−0.92** (0.73)
1922–2010	−0.37* (0.34)	−0.81* (0.61)
Eurasia		
1922–1969	−0.94* (0.47)	−1.49* (0.43)
1970–2010	−0.93* (0.60)	−0.94** (0.45)
1922–2010	−0.91* (0.55)	−1.09* (0.49)
Northern Hemisphere		
1922–1969	−1.69* (0.51)	−2.36* (0.41)
1970–2010	−1.53* (0.46)	−1.83* (0.40)
1922–2010	−1.44* (0.50)	−2.00* (0.49)

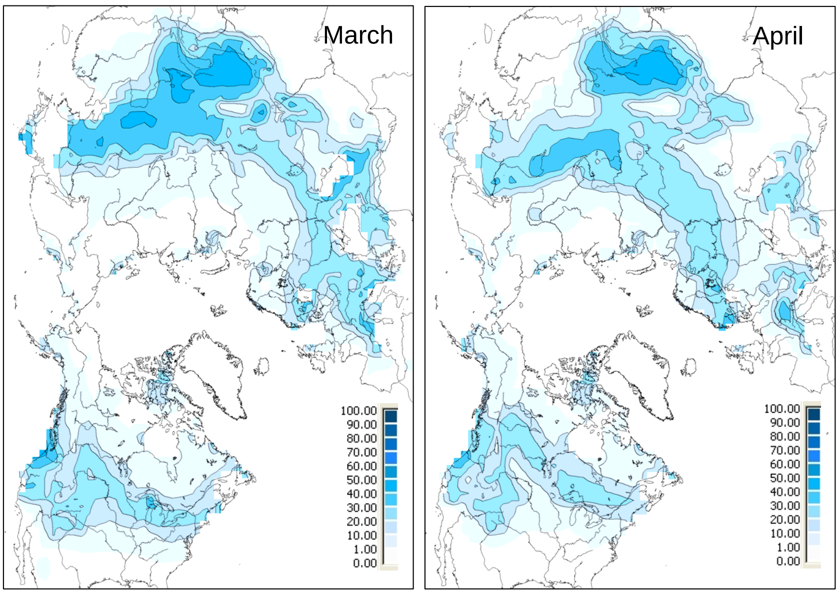

Fig. 1. Standard deviation in mean (1979–2002) March and April snow cover fraction (%) for the six datasets with data in the 1979–2002 overlap period (see Table 2).

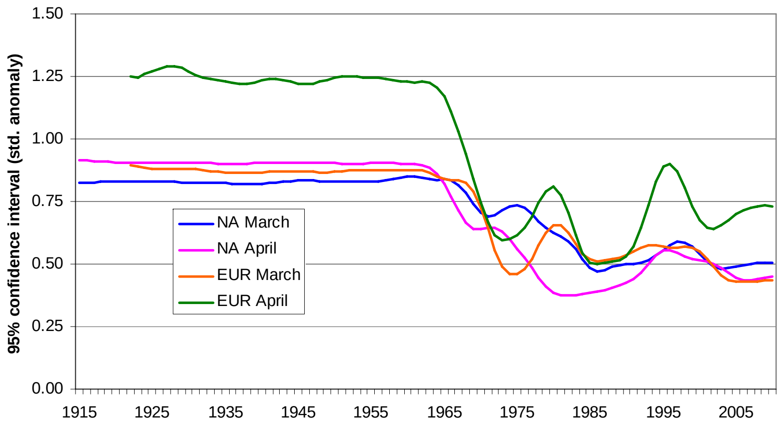

Fig. 2. Smoothed (13-term binomial filter) values of the 95% confidence interval in standardized SCE anomalies computed from the two methods outlined in Sect. 3.

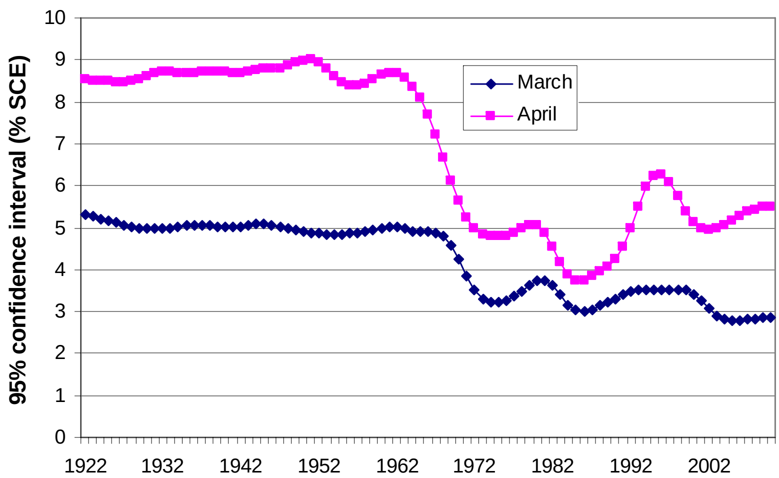

Fig. 3. Smoothed (13-term binomial filter) 95% confidence intervals for NH March and April SCE expressed as a % of the corresponding mean SCE.

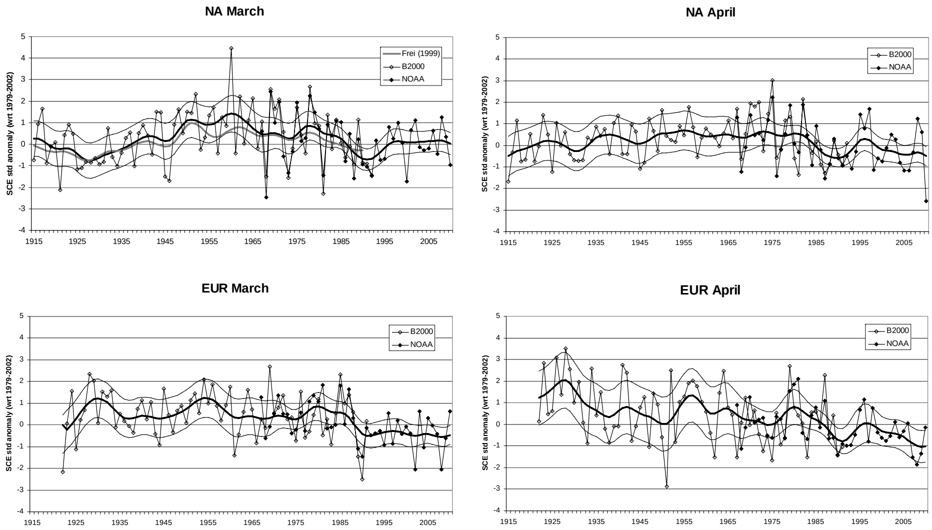

Fig. 4. Variability in NA and EUR March (left) and April (right) SCE anomalies over the period of available data with 13-term filtered values of the mean and 95% confidence interval. The grey smoothed line in NA March is filtered values of the Frei et al. (1999) reconstruction. The width of the smoothed confidence interval is also influenced by the interannual variability in SCE.

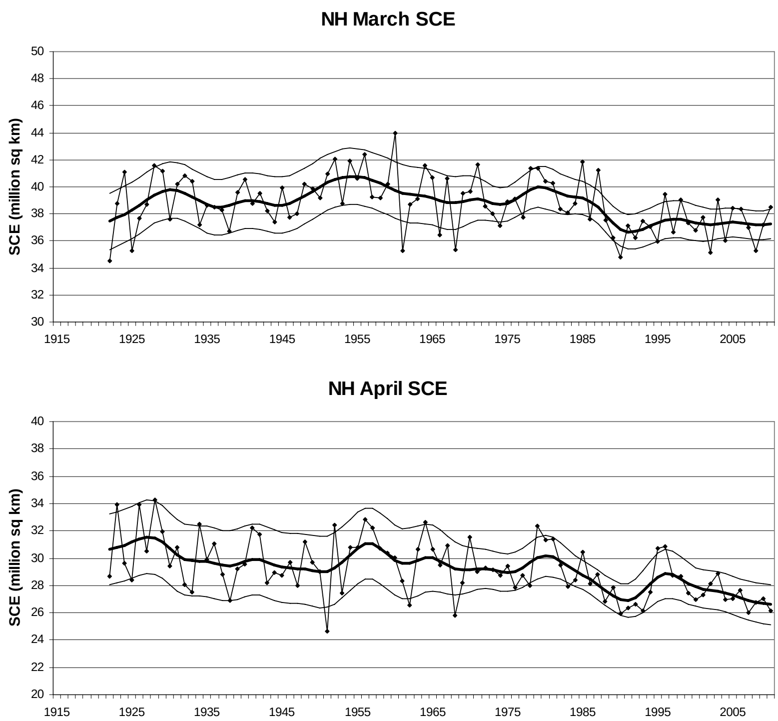

Fig. 5. Same as Fig. 4 for NH SCE estimated from the anomaly series using the NOAA 1979–2002 reference period mean and standard deviation (excludes Greenland which averages 2.16×10^6 km^2).

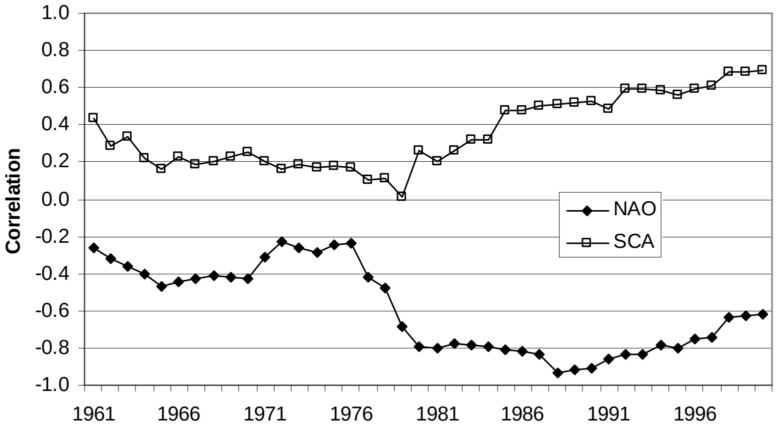

Fig. 6. Running 21-year correlations between the NAO and SCA modes of NH winter (JFM) circulation and NH March SCE. Correlations exceeding 0.4 are nominally significant at a 0.05 level assuming data series are not autocorrelated.

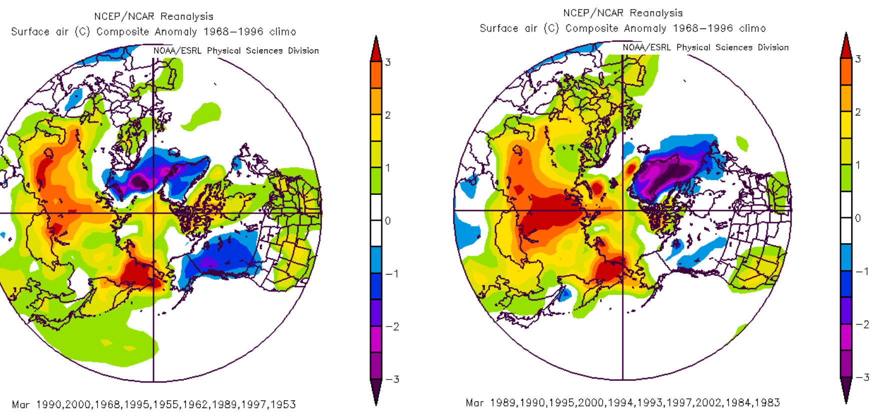

Fig. 7. Average March surface air temperature anomalies from the NCEP reanalysis for the 10 winters in the 1951–2010 period with the most negative values of the SCA index (left) and the most positive values of the NAO index (right). The plots were generated using the online composite plotting tool at http://www.esrl.noaa.gov/psd/cgi-bin/data/composites/printpage.pl.

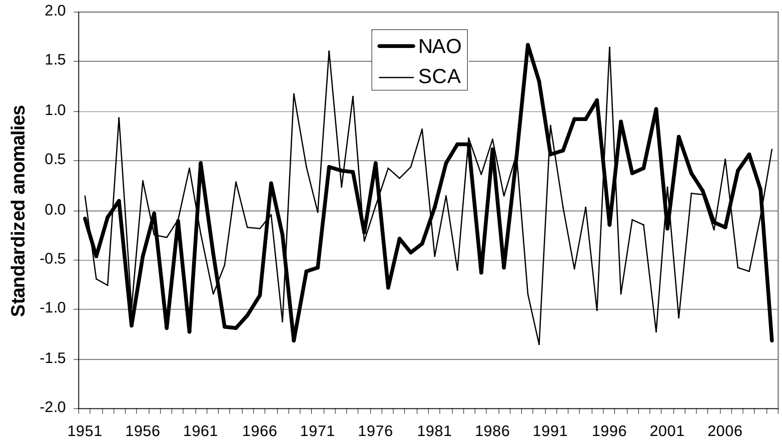

Fig. 8. Variation in standardized anomalies of winter (January–March) values of the NAO and SCA indices over the period from 1951 to 2010 as computed by the NOAA Climate Prediction Center.

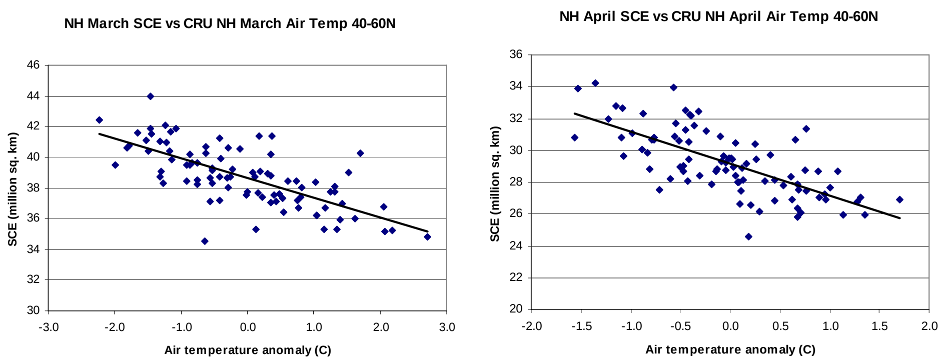

Fig. 9. Relationship between NH March and April SCE and corresponding land area air temperature anomalies over 40–60° N from the CRU dataset. The amount of variation explained by air temperature was 49.6% and 48.7% for March and April, respectively.

Discussion Paper | Discussion Paper | Discussion Paper | Discussion Paper |